Supplementary Information

Phytic acid-doped poly-*N*-phenylglycine potato peels for removal of anionic dyes: Investigation of adsorption parameters

Kahina Bouhadjra[a,b,c], Alexandre Barras[c], Wahiba Lemlikchi[a,d], Ahmed Addad[e], Manash R. Das[f,g], Mohammed A. Amin,[h] Sabine Szunerits[c] and Rabah Boukherroub[c]*

[a]*Laboratory of Applied Chemistry and Chemical Engineering (LACCE), University of Tizi-Ouzou, Tizi-Ouzou, Algeria*

[b]*High National School of Public Works (HNSPW), El Kouba, Algiers, Algeria*

[c]*Univ. Lille, CNRS, Centrale Lille, Univ. Polytechnique Hauts-de-France, UMR 8520, IEMN, F-59000 Lille, France*

[d]*University of Algiers 1, Algiers, Algeria*

[e]*Univ. Lille, CNRS, UMR 8207 - UMET, F-59000, Lille, France*

[f]*Advanced Materials Group, Materials Sciences and Technology Division, CSIR-North East Institute of Science and Technology, Jorhat, 785006, India*

[g]*Academy of Scientific and Innovative Research, Ghaziabad 201002, India*

[h]*Department of Chemistry, College of Science, Taif University, P.O. Box 11099, Taif 21944, Saudi Arabia*

Materials and methods

N-phenylglycine monomer, *N*-phenyl-*p*-phenylenediamine, phytic acid (50% wt/wt in H_2O) and ammonium persulfate (APS) were provided from Sigma-Aldrich. Potato peels waste was obtained from a restaurant in Tizi-Ouzou, Algeria. Two commercial anionic dyes (Fig.S1) were used as adsorbates in the experiments. Reactive blue 49 (RB 49) and direct blue 199 (DB 199) dyes, supplied by DBK textile industry, Tizi-Ouzou, (Algeria), are used as-received without further purification. RB 49 is anthraquinone dye with molecular weight of 882.18 g/mol and its molecular formula is $C_{32}H_{23}ClN_7Na_3O_{11}S_3$. DB 199 is phthalocyanine dye with molecular weight of 775.20 g/mol and its molecular formula is $C_{32}H_{18}CuN_9NaO_6S_2$ (Fig.S1).

Characterization

The zeta potential study was performed using a zeta sizer Malvern (ZSP). The thermal degradation characteristics of the adsorbents were studied under nitrogen flow using a thermogravimetric method. Experiments were performed on a Netzsch, TG 209 F3 Tarsus analyzer. Scanning electron microscopy (SEM) images were recorded using a JEOL microscope FEG-SEM JSM 6330F operated at 1 kV. Fourier-transform infrared spectroscopy (FTIR) was carried out to identify the functional groups of the composites using a Nicolet8700 FTIR spectroscopy. Raman spectroscopy measurements were conducted on LabRam-HR Micro-Raman system (Horiba France) using a 473 nm Laser diode as excitation source. Visible light is focused by a 1800 mm focal length monochromator and detected by a CCD camera. X-ray photoelectron spectroscopy (XPS) was performed by XPS SpecslabII (Phoibos-Hsa 3500 150, 9 channeltrons) SPECS spectrometer. The specific surface area was determined by the nitrogen gas adsorption study at 77K using a QuantachromeASIQ-win surface area analyzer and Brunauer-Emmett-Teller (BET) calculations. The concentration of RB49 and DB 199 dyes was analyzed by using UV-visible spectrophotometer (Perkin- Elmer Lambda950).

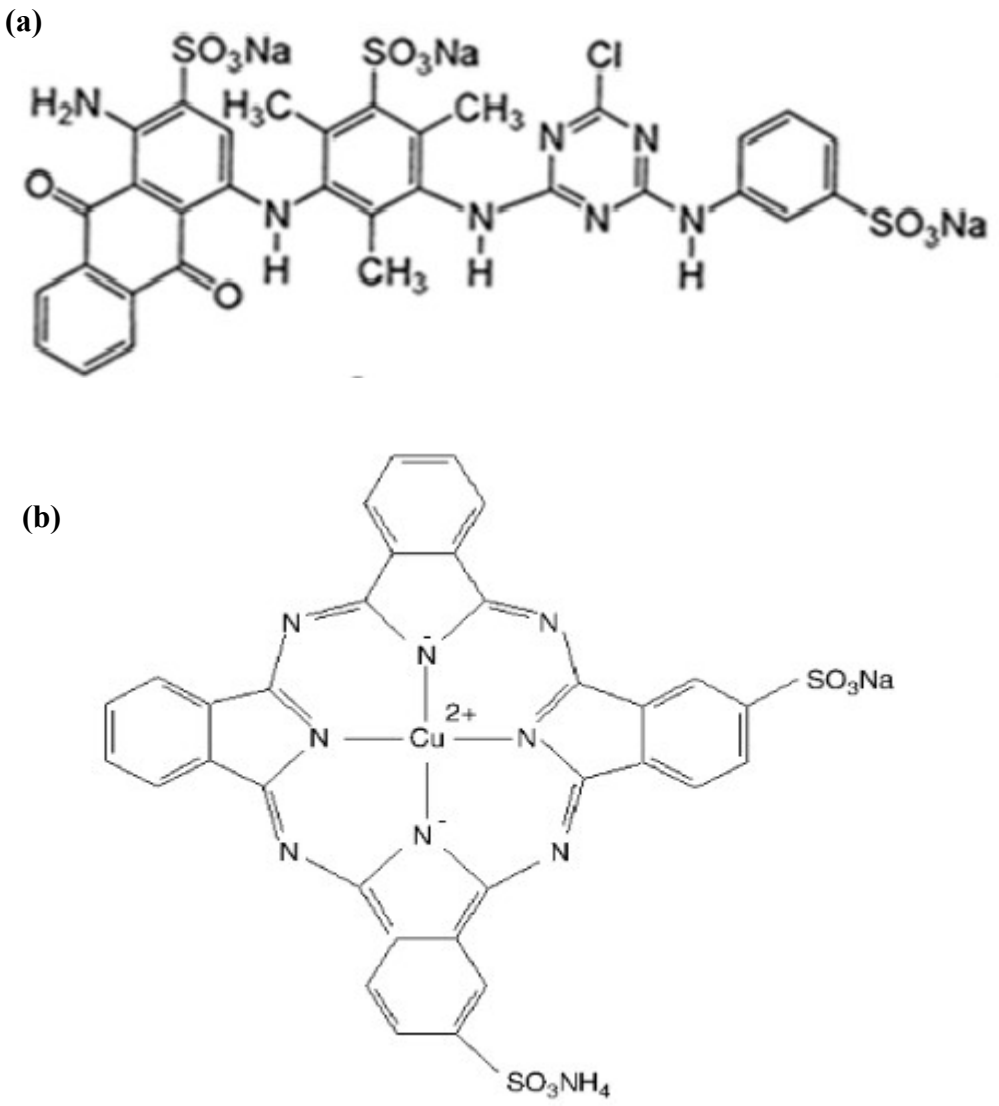

Figure S1. Chemical structure of (**a**) reactive blue 49 and (**b**) direct blue 199.

Chemical name	**Commercial name**	**Chemical class**	**Molecular weight (g/mole)**	**Chemical formula**	**λ (nm)**
(a) Reactive blue 49	*Cibacron Blue P- 3R*	Reactive anthraquinone	882.18	$C_{32}H_{23}ClN_7Na_3O_{11}S_3$	625
(b) Direct blue 199	*Turquoise Blue BRLE*	Direct phthalocyanine	775.20	$C_{32}H_{18}CuN_9NaO_6S_2$	610

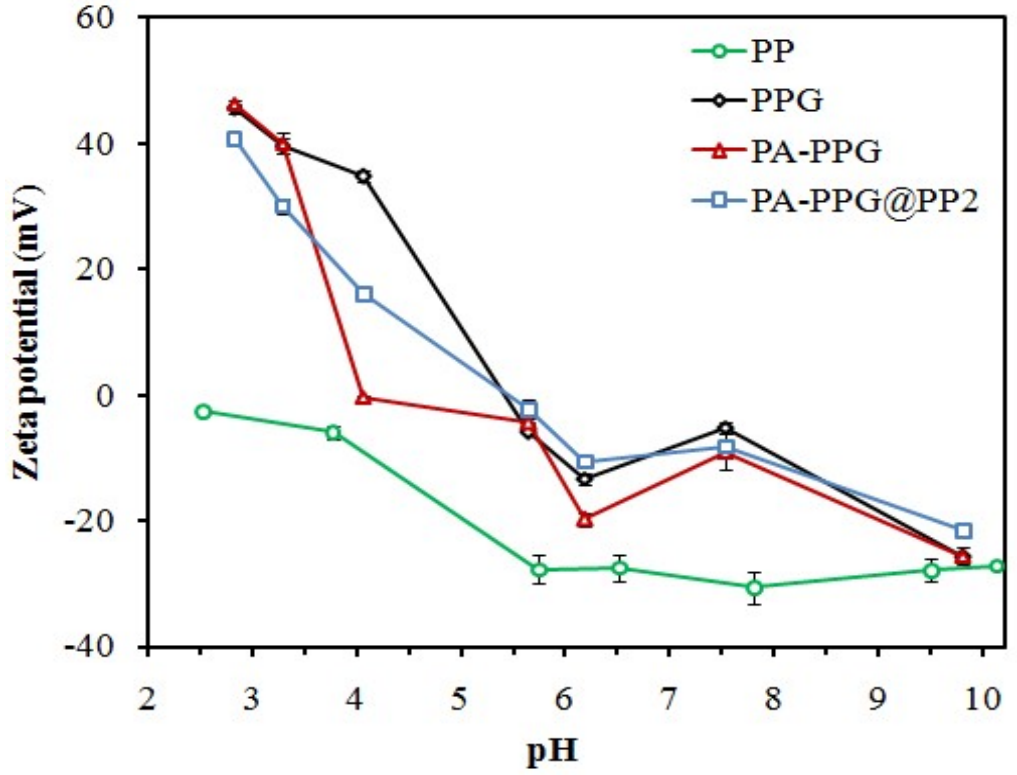

Figure S2. Effect of solution pH on zeta potential of PP (green), PPG (black), PA-PPG (red), and PA-PPG@PP2 (blue).

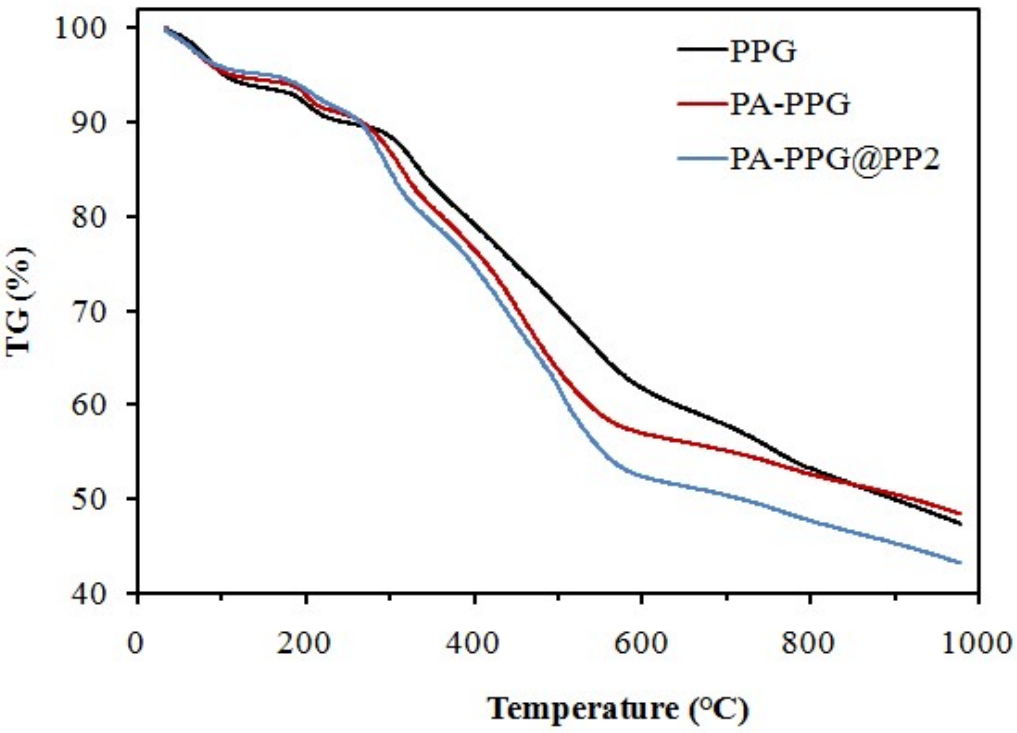

Figure S3. Thermogravimetric analysis of PPG (black), PA-PPG (red), and PA-PPG@PP2 (blue).

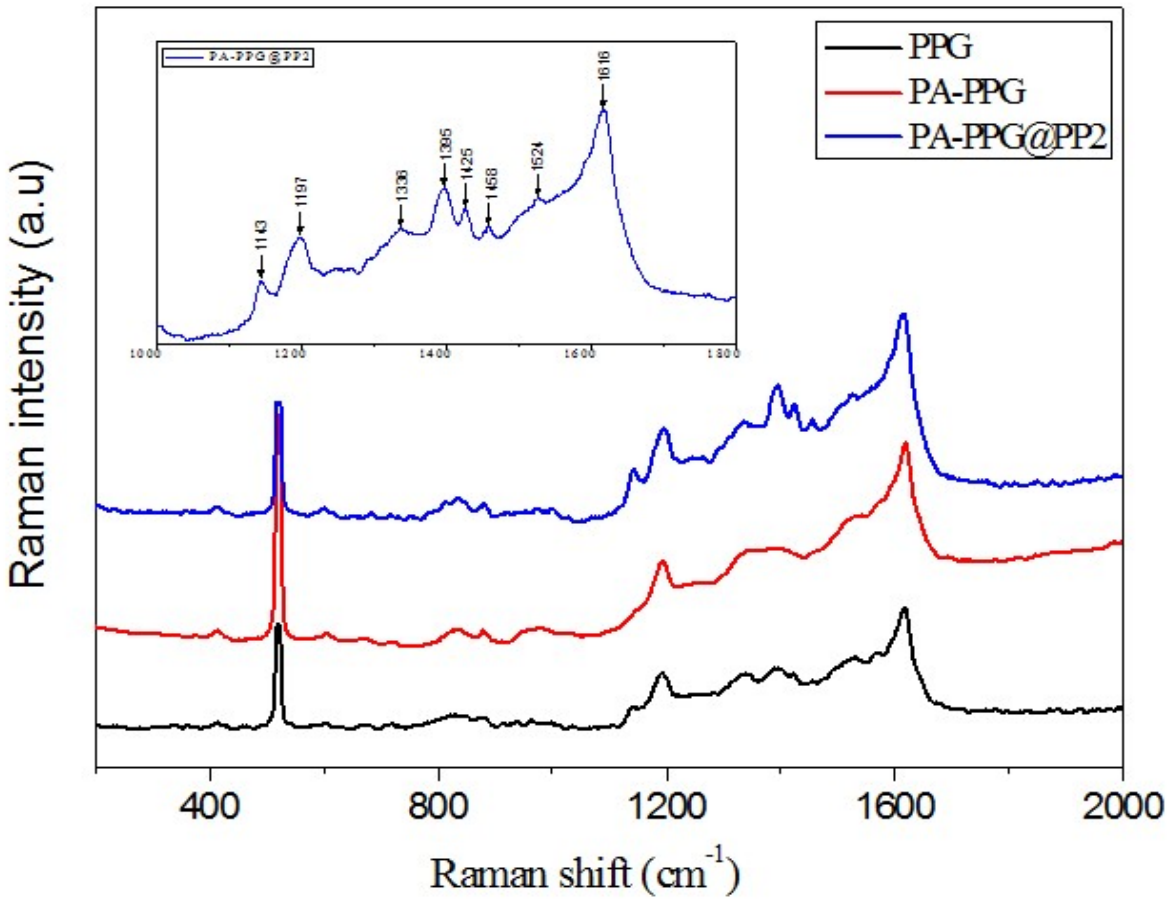

Figure S4. Raman spectra of PPG (black), PA-PPG (red) and PA-PPG@PP2 (blue).

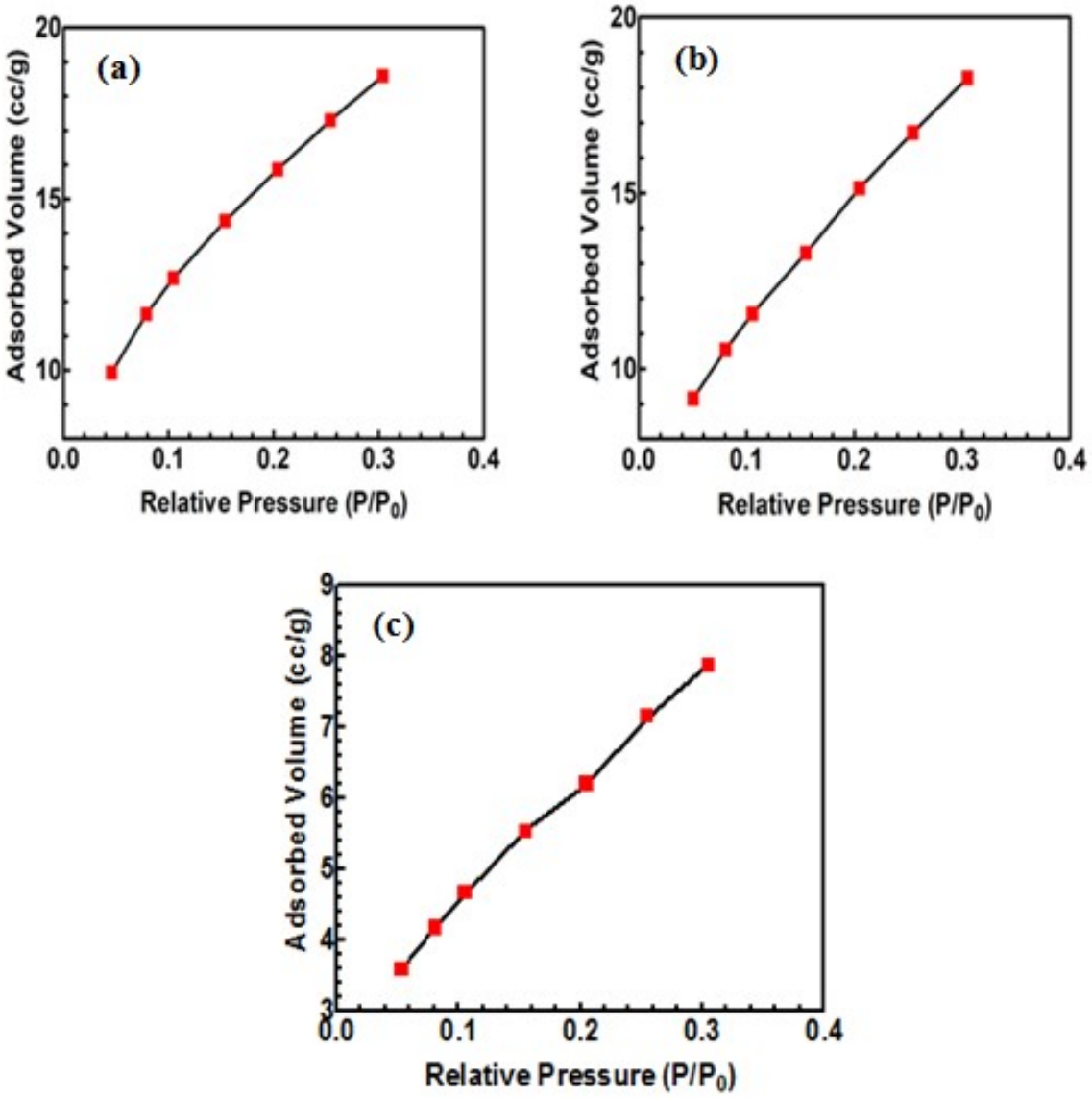

Figure S5. BET isotherm plots of (**a**) PPG, (**b**) PA-PPG, and (**c**) PA-PPG@PP2.

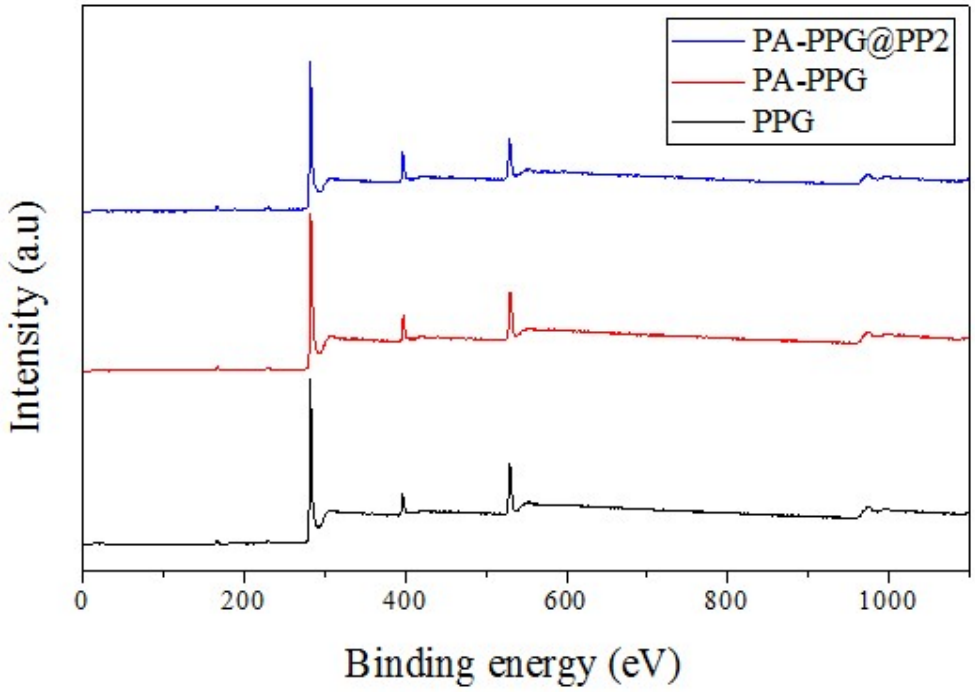

Figure S6. X-ray photoelectron spectroscopy (XPS) survey spectra of PPG (black), PA-PPG (red) and PA-PPG@PP2 (blue).

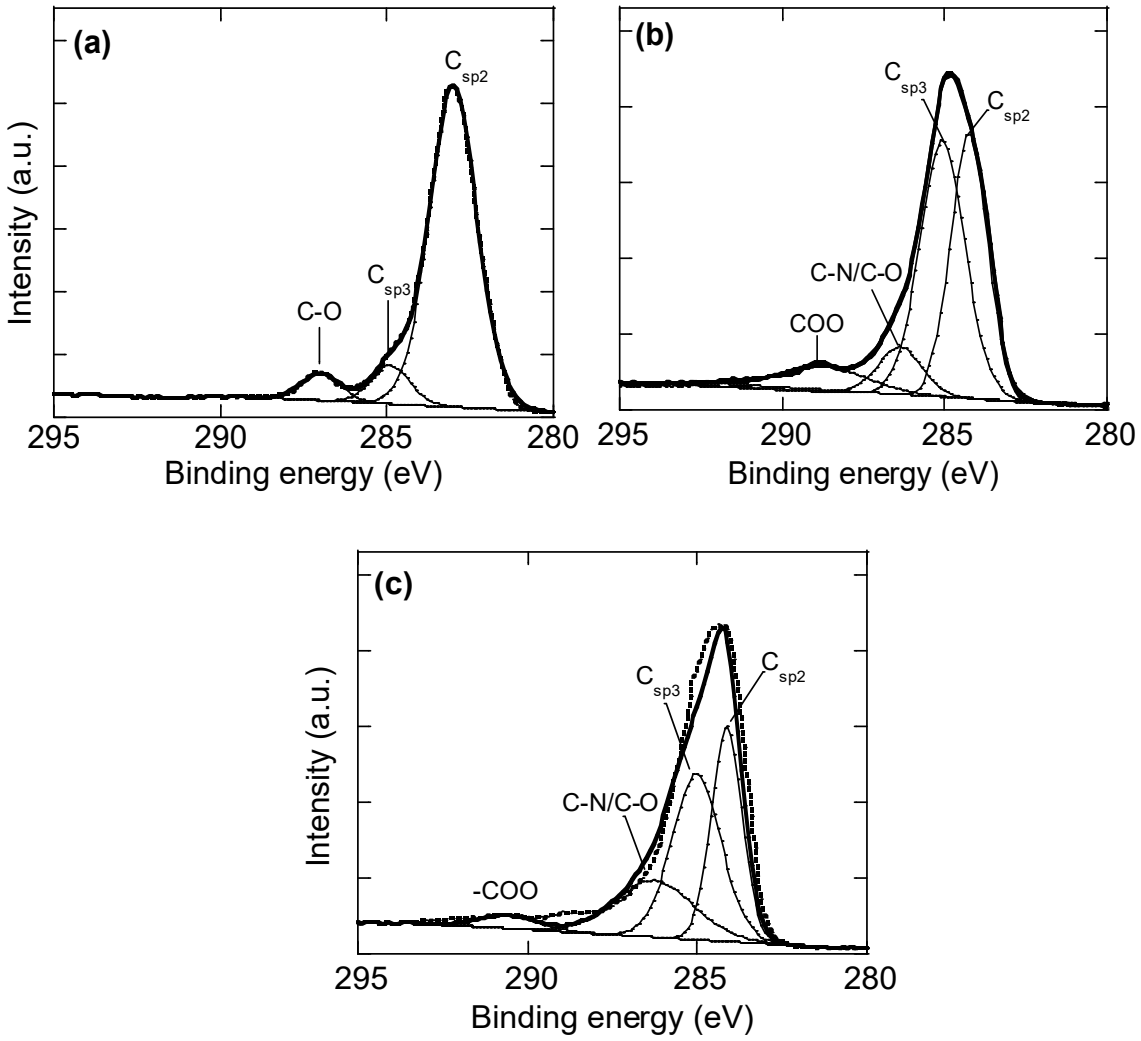

Figure S7. High-resolution XPS spectra of the C1s of (**a**) PPG, (**b**) PA-PPG, and (**c**) PA-PPG@PP2.

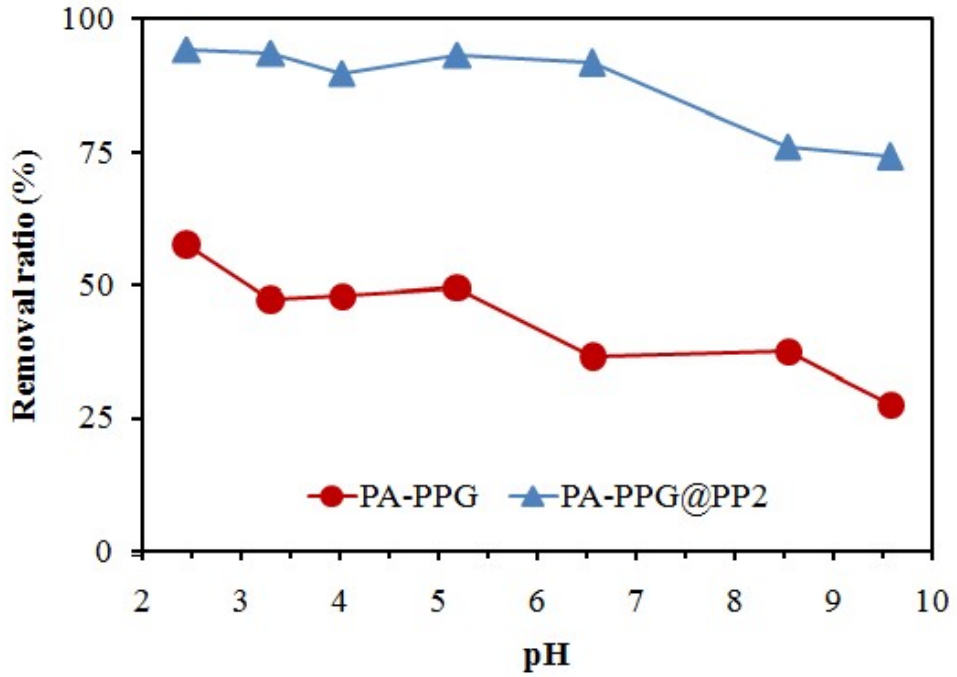

Figure S8. Effect of solution pH on adsorption of RB 49 onto PA-PPG (100 mg/L) and PA-PPG@PP2 (100 mg/L), adsorbent dose=0.5 g/L, t=2 h and T=25 °C.

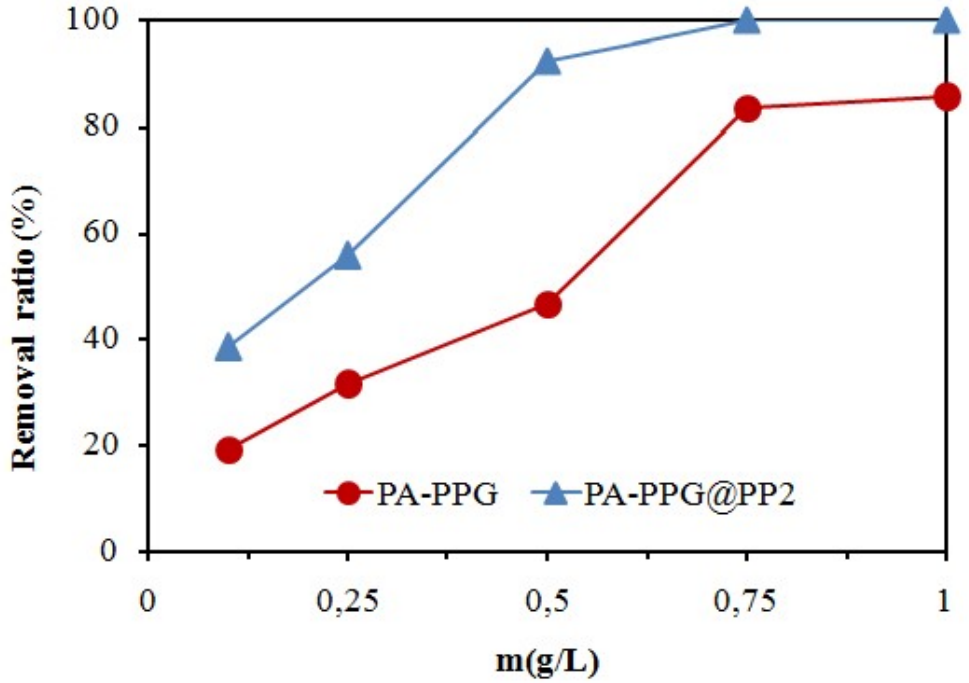

Figure S9. RB 49 adsorption ratio as a function of PA-PPG and PA-PPG@PP2 dose (pH=6.5, [RB49]=100 mg/L, adsorption time=24 h and T=25 °C).

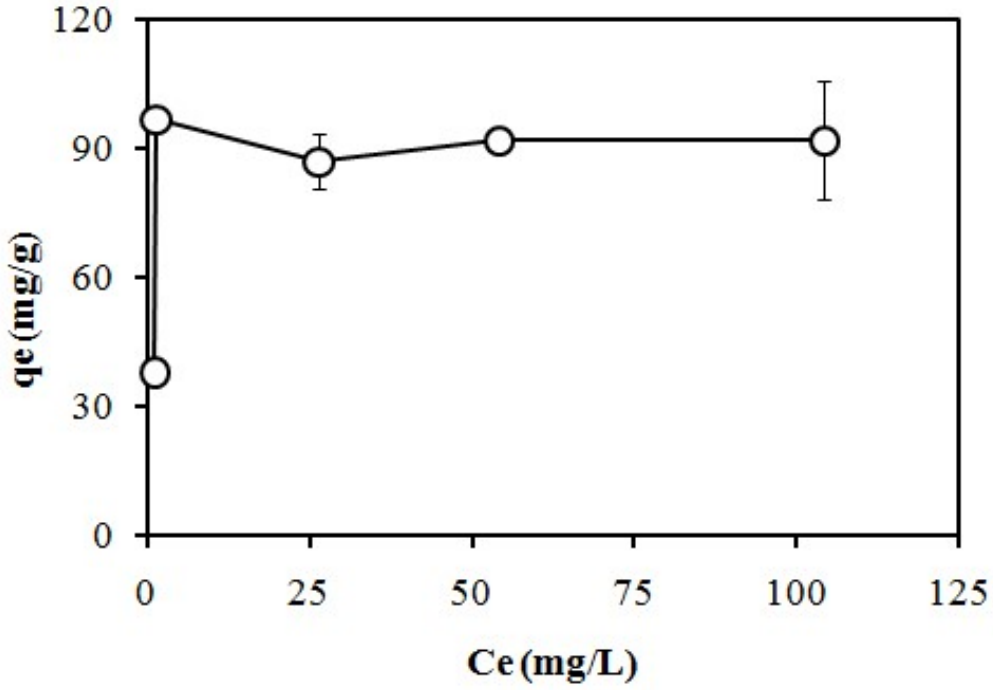

Figure S10. Isotherm plot for the adsorption of RB 49 onto PA-PPG (pH = 6.5, adsorbent dose=0.5 g/L, t=24 h and T=25 °C).

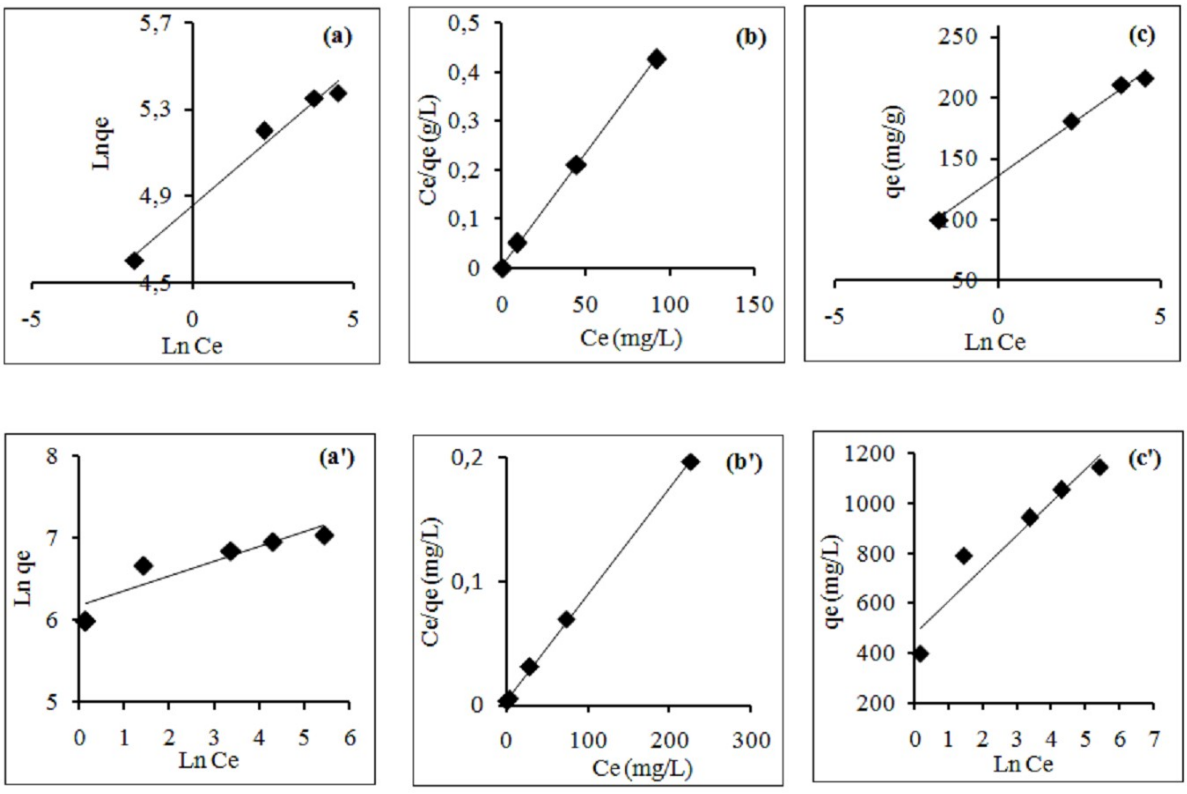

Figure S11. Adsorption isotherm curves recorded at 298 K fitted to (**a, a'**) Freundlich, (**b, b'**) Langmuir and (**c, c'**) Temkin models for RB 49 (top) and DB 199 (bottom).

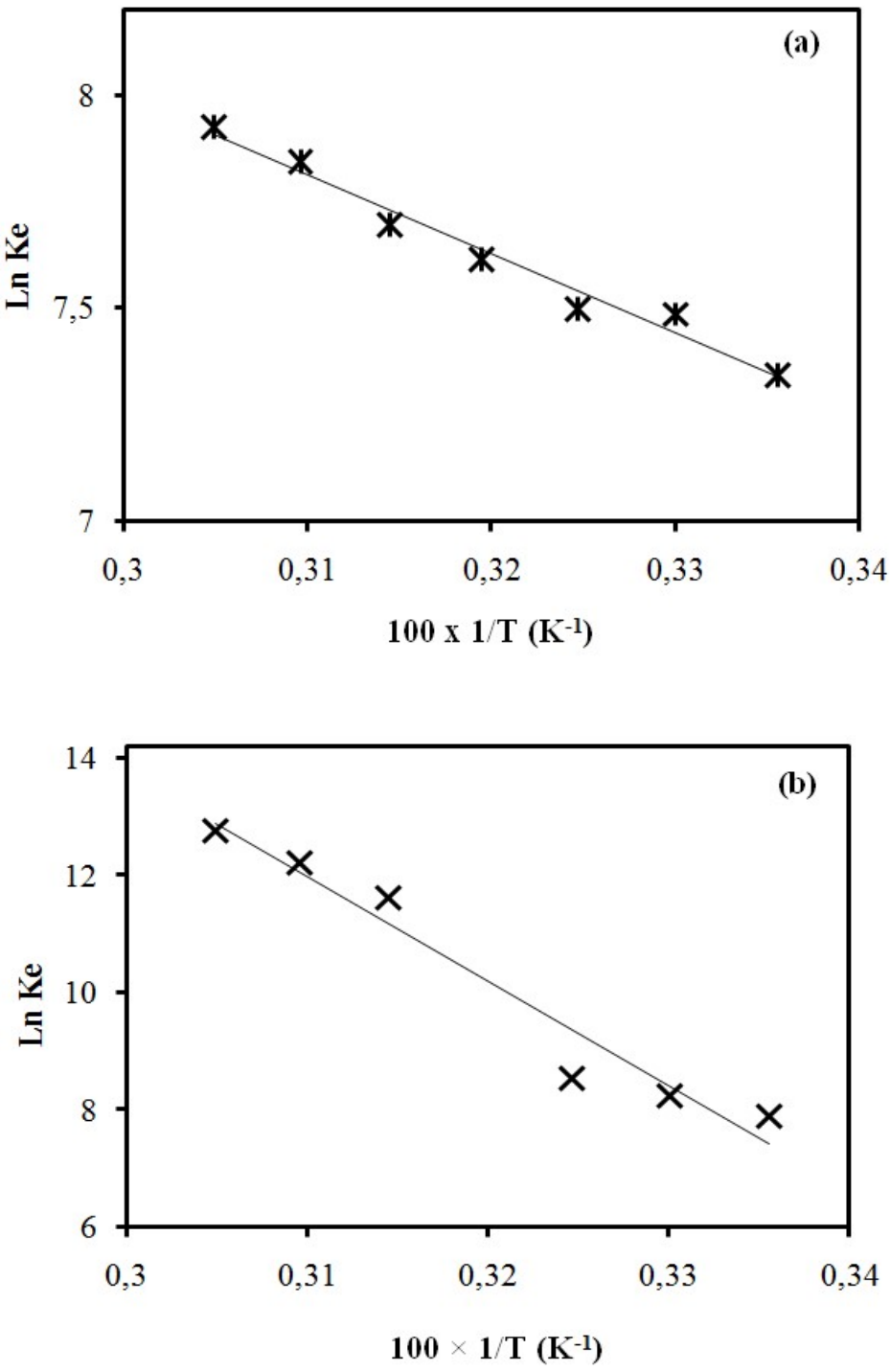

Figure S12. Thermodynamic parameters of adsorption of RB 49 (**a**) and DB 199 (**b**) onto PA-PPG@PP2 using Van't Hoof equations, (pH=6.5, adsorbent dose=0.5 g/L, t=3 h, [RB49]=200 mg/L and [DB 199]=400 mg/L).

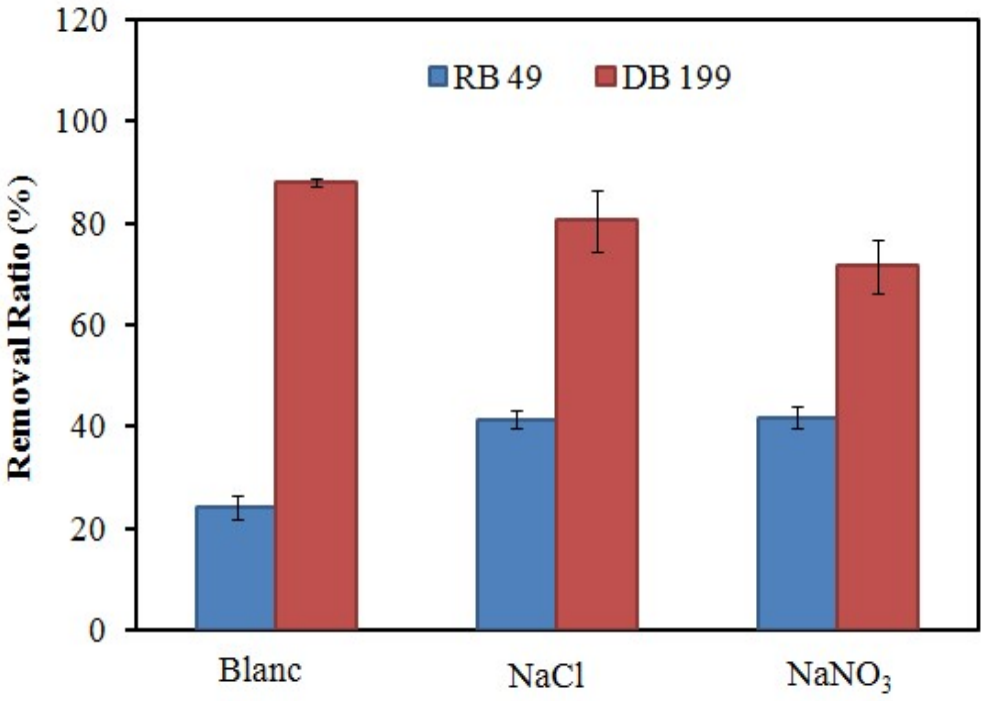

Figure S13. Adsorption of RB 49 and DB 199 on PA-PPG@PP2 in presence of anionic species, (pH = 6.5, adsorbent dose = 0.5 g/L, T=25 °C, [RB49] = 200 mg/L, [DB 199] = 400 mg/L, [anionic species] = 0.05M).

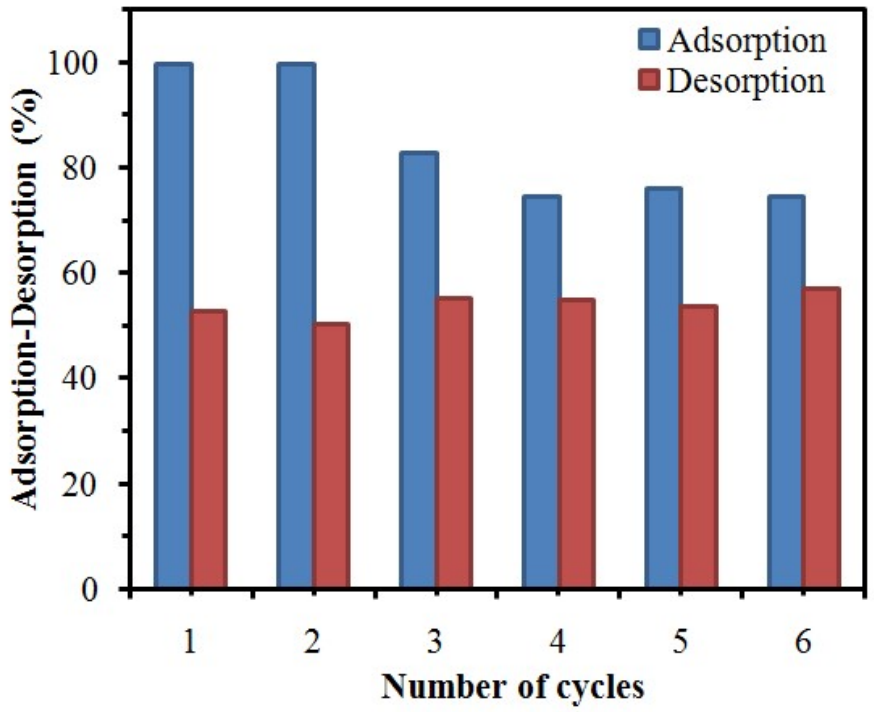

Figure S14. Removal efficiency of the PA-PPG@PP2 after six successive cycles of adsorption–desorption DB 199 (adsorbent dose = 0.5 g/L, [DB 199] = 200 mg/L, T=55 °C, t=60 min).

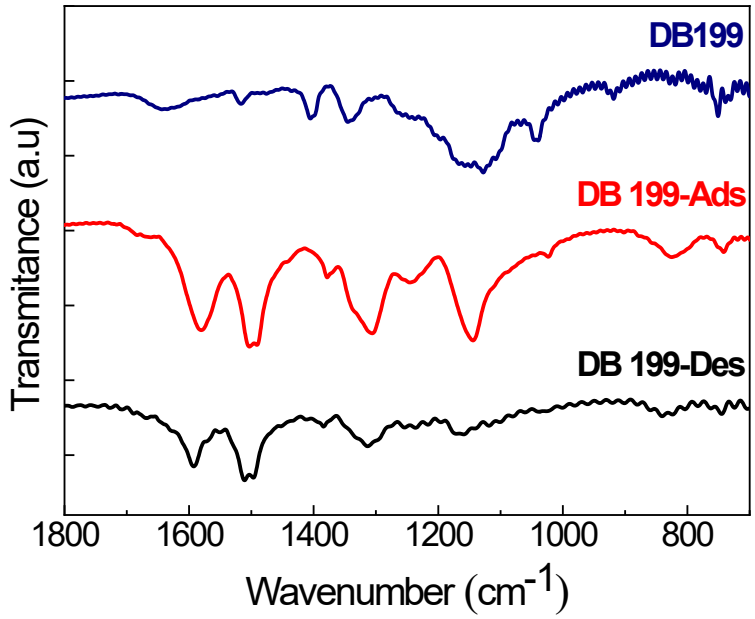

Figure S15. FTIR spectra of DB 199 dye and PA-PPG@PP2 after DB 199 dye adsorption/desorption (pH=6.5, adsorbent dose=0.5 g/L, [DB 199]=200 mg/L, T=55 °C, contact time: 60 min).

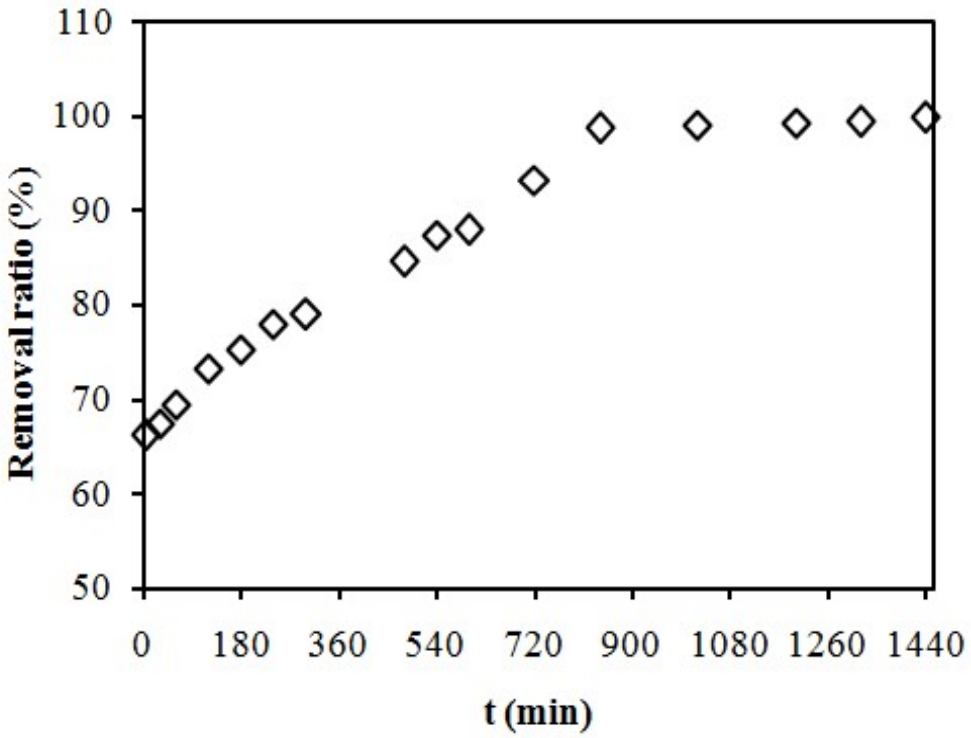

Figure S16. Effect of contact time on the adsorption of DB 199 dye onto PA-PPG@PP2 (pH=6.5, adsorbent dose=0.5 g/L, [DB 199]=400 mg/L, T=25 °C).

Table S1. Attribution of the main FTIR bands' frequencies.

Wavenumber (cm^{-1})			**Attribution**
PPG	PA-PPG	PA-PPG@PP2	
1692	1688	-	bending vibration of carboxyl groups C=O
1579	1582	1586	quinone ring stretching deformations
1494	1492	1495	benzene ring stretching deformations
1313	1314	1314	C-N stretching vibration of benzenoid amine
1253	1254	1252	C=N stretching vibrations
1155	1154	1154	C–O–C asymmetrical stretching
827	829	826	Benzene ring deformation
750	749	749	bending vibrations of C–H bonds

Table S2. Physical characteristics of the adsorbent materials.

Adsorbent	**Surface area (m^2/g)**	**Pore volume (cm^3/g) $\times 10^{-2}$**	**Pore diameter (Å)**
PPG	59	2.9	19
PA-PPG	60	2.8	19
PA-PPG@PP2	26	1.2	19

Table S3. Elemental composition of the developed adsorbent materials determined from XPS analysis.

	C_{1s} (at.%)	O_{1s} (at.%)	N_{1s} (at.%)	S_{2p} (at.%)	P_{2p} (at.%)
PPG	83.59	9.73	5.92	0.76	-
PA-PPG	82.71	9.69	6.56	0.89	0.15
PA-PPG@PP	81.79	8.02	8.79	1.04	0.36

Table S4. Kinetic parameters for the adsorption of RB 49 and DB 199 onto PA-PPG@PP2 at different temperatures.

Adsorbent	T (K)	Pseudo-first-order				Pseudo-second-order			Intra-particle diffusion					
		$q_{e,\ exp}$ (mg/g)	$q_{e,\ cal}$ (mg/g)	K_1 (1/mn)	R^2	$q_{e,\ cal}$ (mg/g)	K_2 g/ (mg.min)	R^2	$K_{id,\ 1}$ (mg/g. $min^{0.5}$)	C (mg/g)	R^2	$K_{id,\ 2}$ (mg/g. $min^{0.5}$)	C (mg/g)	R^2
RB 49	298	185	24.09	0.02	0.847	182	0.004	0.999	1.549	161.9	0.901	-	-	-
	303	192	21.67	0.01	0.965	196	0.005	0.999	3.452	166.6	0.935	1.212	178.2	0.992
	318	200	15.84	0.02	0.920	200	0.006	0.999	3.680	173.4	0.997	0.818	189.2	0.970
	328	186	10.23	0.01	0.440	189	0.010	0.999	6.233	154.6	0.986	0.314	184.7	0.453
DB 199	298	553	153.83	0.01	0.903	556	2.4×10^{-4}	0.999	6.724	436.6	0.991	-	-	-
	303	603	145.21	0.05	0.938	625	1.95×10^{-4}	0.999	16.35	404.1	0.955	5.560	506.5	1.000
	318	797	165.95	0.05	0.700	833	1.75×10^{-4}	0.999	35.23	449.7	0.963	1.171	777.9	0.809
	328	798	74.13	0.02	0.269	833	6×10^{-4}	0.999	79.56	284.9	0.923	0.188	794.4	0.175

Table S5. Comparison of maximum adsorption capacities of various adsorbents towards RB 49 and DB 199 dyes.

Adsorbent	Pollutant	Adsorption capacity, q_{max} (mg/g)	Reference
Citrus waste biomass (raw)	RB 49	135.16	[1]
Citrus waste biomass (immobilized)	RB 49	80.00	[1]
Citrus waste biomass (Acetic acid treated)	RB 49	232.56	[1]
Mixed biosorbent (ABTOC)	RB 49	151.05	[2]
Capsicum annuum seeds (acetone treated)	DB 199	96.35	[3]
Waste Biomass of *Aspergillus fumigatus*	DB 199	60.6	[4]
A. niger powder	DB 199	29.96	[5]
maize cob, *citrus* peel and rice husk powders	DB 199	18.58	[6]
Cucurbit [6] uril (CB [6])	DB 199	240	[7]
PAn/γ-Al_2O_3nanocomposite	DB 199	1000	[8]
$Ti_{0.95}Fe_{0.05}O_2$	RB 49	100% (degradation)	[9]
TiO_2 nanoparticles		99.33% (degradation)	[10]
Phytic acid-doped PPG		92	**This work**
Phytic acid-doped PPG@PP2	RB 49	216 (T = 298 K), 285 (T = 318 K)	**This work**
Phytic acid-doped PPG@PP2	DB 199	1148 (T=298K)	**This work**

Table S6. Thermodynamic parameters of adsorption of RB 49 and DB 199 onto PA-PPG@PP2.

Adsorbate	**ΔG° (KJ/mol)**							**ΔH° (J/mol)**	**ΔS° (J/mol.K)**
	298K	303K	308K	313K	318K	323K	328K		
RB 49	-18.19	-18.85	-19.20	-19.82	-20.56	-21.06	-21.60	+153.92	+112.65
DB 199	-19.55	-20.79	-21.90	-22.43	-30.71	-32.85	-34.80	+1484.88	+559.86

References

1. M. Asgher and H. N. Bhatti, *Can. J. Chem. Eng.*, 2012, **90**, 412-419.
2. S. T. Akar, A. Gorgulu, Z. Kaynak, B. Anilan and T. Akar, *Chem. Eng. J.*, 2009, **148**, 26-34.
3. S. T. Akar, A. Gorgulu, T. Akar and S. Celik, *Chem. Eng. J.*, 2011, **168**, 125-133.
4. B. Wang, K. Zhou, H. Liu and W. Z. Tang, *Environ. Process*, 2016, **3**, 843-856.
5. X. J. Xiong, X. J. Meng and T. L. Zheng, *J. Hazard. Mater.*, 2010, **175**, 241-246.
6. S. Saroj, S. V. Singh and D. Mohan, *Arab. J. Sci. Eng.*, 2015, **40**, 1553-1564.
7. Y. A. Patil, B. Sadhu, D. R. Boraste, A. L. Borkar and G. S. Shankarling, *J. Mol. Struct.*, 2020, **1202**, 127278.
8. H. Javadian, M. T. Angaji and M. Naushad, *J. Ind. Eng. Chem.*, 2014, **20**, 3890-3900.
9. S. Saroj, L. Singh, R. Ranjan and S. V. Singh, *Res. Chem. Intermed.*, 2019, **45**, 1883-1906.
10. L. Singh, S. Saroj, Y. Lee and S. V. Singh, *J.Mater. Sci.*, 2016, **27**, 2581-2588.